Journal of the Meteorological Society of Japan, Vol. 83, No. 1, pp. 89–106, 2005

The Rainfall Phenomena during the Pre-monsoon Period over the Indochina Peninsula in the GAME-IOP Year, 1998

Masashi KIGUCHI and Jun MATSUMOTO

Department of Earth and Planetary Science, University of Tokyo, Tokyo, Japan

(Manuscript received 27 July 2004, in final form 28 October 2004)

Abstract

The rainfall phenomena in the pre-monsoon season over the Indochina Peninsula are investigated using geopotential height, wind and moisture fields by the NCEP/NCAR reanalysis, and OLR, precipitation and GPS data during the GAME-IOP year, 1998. In early and middle April, and early May, the lower OLR regions, which represent the heavy convective activity, extend southward from the mid-latitude zone to the Indochina Peninsula, bringing intermittent rainfall events in a wide region over the central part of the peninsula. The composite analysis in these three rainfall events shows that they are brought by the trough passage in the upper troposphere, which migrates eastward in the middle latitude westerlies along the southern periphery of the Tibetan Plateau. The lower tropospheric moisture inflow in these rainfall events is found to come mainly from the south and east, which shows sharp contast with the situations of inflow mainly from the west, during the non-precipitation days in the pre-monsoon season, and the rainfall situations after the monsoon onset in middle May.

1. Introduction

It is well known that the Asian summer monsoon (hereafter ASM) is characterized by wind system and abundant rainfall. The wind system has strong vertical shear between the lower and upper troposphere. In summer, the prevailing wind direction in the lower and upper troposphere from India to the South China Sea is westerly and easterly, respectively. Rainfall amount during summer occupies a high ratio of the annual precipitation. Climatological features of the onset of the wind system and rainy season, and the subsequent seasonal march, however, change greatly with regions (Matsumoto 1992).

It is generally recognized that the initial onset stage of the ASM is characterized by the establishment of strong convection, and the change of the prevailing wind direction in the Bay of Bengal, the Indochina Peninsula and the South China Sea in early or middle May (He et al. 1987; Matsumoto 1992; Murakami and Matsumoto 1994; Lau and Yang 1997; Wu and Zhang 1998; Hsu et al. 1999).

In the previous studies, various methods have been proposed to determine the monsoon onset. Firstly, rainfall or convective activity indicated by satellite observation is used (e.g., Ananthakrishnan and Soman 1988; Lau and Yang 1997; Wang and LinHo 2002). The well known onset map in India (India Meteorological Department 1943) was depicted based on the rainfall data. Second, the wind field has been utilized (e.g., Orgill 1967; Holland 1986; Cheang and Tan 1988; Wang et al. 2004). In addition, there were studies using a combination of both rainfall or convective activity and wind field (e.g., Ahmed and Karmakar 1993; Xie et al. 1998). Recently, Fasullo and Webster (2003) studied the onset and withdrawal dates of the Indian monsoon, derived from variability in the large-scale hydrologic cycle.

Corresponding author: Masashi Kiguchi, Graduate School of Science, Kyoto University, Japan 606-8502, COE Research fellow
E-mail: kiguchi@kugi.kyoto-u.ac.jp

There are very few studies of the monsoon onset in the Indochina Peninsula compared with those on India. The onset maps of the rainy season over the whole monsoon region by Kurashima (1959), Ramage (1971), and Tao and Chen (1987) were all based on several studies applying different onset criteria. In such preceding maps, no information was presented in the inland region of the Indochina Peninsula. Recently, some studies present onset and retreat of summer rainy season by using satellite derived cloud data (e.g., Tanaka 1992; Murakami and Matsumoto 1994). According to these studies, the onset of the summer rainy season over the Indochina Peninsula is shown to be ahead of the advance of the monsoon rainfall over South India. More than 50 years ago, Yin (1949) tried to explain why summer monsoon rainfall arrives earlier in Burma than in India.

The appearance of strong convection over the Indochina Peninsula, indicative of the earliest start of the summer monsoon over the Asian continent, has been documented in some recent studies (e.g., Lau and Yang 1997; Webster et al. 1998; Wang and LinHo 2002). According to these studies, the monsoon onset over the Indochina Peninsula occurs in early or middle May, and migrates northward from the southern part of the Bay of Bengal. On the other hand, Matsumoto (1997) pointed out that the onset of rainy season occurs earlier in late April in the inland region over the Indochina Peninsula, when Indochina is still under a mid-latitude westerly regime. The full summer monsoon circulation begins in middle May, concurrent with the onset of the rainy season in the coastal region along the Bay of Bengal. When the pentad number in each grid shown by Wang and LinHo (2002) is examined, there is one grid in the northern part of Thailand, where the onset occurs earlier in Pentad 25 than that in the neighboring part in Pentad 27–29, implying earlier rainy season onset there. However, the contour lines of the onset date in this study do not display the earlier onset of rainy season in the inland area of the Indochina Peninsula.

The monsoon onset in each year in Thailand, located in the central part of the Indochina Peninsula, was defined by Zhang et al. (2002) using the rainfall index. The mean onset date for 46 years is 9 May. After one pentad later, the northward progression of the southwesterly flow in the equatorial Indian Ocean is clearly identified. This also shows that the monsoon onset derived by the rainfall index occurs before the establishment of monsoon circulation. All these studies show the discrepancies between the onset defined by rainfall and wind. The property of such rainfall before the establishment of monsoon circulation, however, has not been revealed yet.

It is known that the convective activity or rainfall prior to the monsoon circulation (hereafter called pre-monsoon rain) is seen in the region from the southern edge of the Tibetan Plateau to the Gulf coast of Bengal, including the northeastern part of India, Bangladesh, and Nepal (Rao and Boothalingam 1957; Koteswaram and Srinivasam 1958; Ahmed 1989; Baral and Mackerras 1992). On the other hand, the pre-monsoon rains over the Indochina Peninsula have been hardly researched, except for climatological descriptions by Nieuwolt (1981).

The objective of this study is to investigate the characteristics of the pre-monsoon rains prior to the monsoon onset over the Indochina Peninsula during the GAME-IOP (GEWEX Asian Monsoon Experiment—Intensive Observation Period) year, 1998, when various meteorological data were collected in the Indochina Peninsula.

2. Dataset

In order to know the rainfall distribution in the inland region of the Indochina Peninsula, the daily rainfall data of stations observed and archived by the meteorological agencies in Thailand, Laos and Cambodia, obtained by the GAME-Tropics dataset are used (Agata 2002). Observation stations are shown in Fig. 1.

Furthermore, the daily mean precipitable water in the atmosphere derived from the Global Positioning System (GPS) observations at Bangkok and Chiang Mai conducted by the GAME-Tropics project in the same year are utilized. Takiguchi et al. (2000) pointed out that there is a strong correlation between a rapid increase of the water vapor content in the zenith direction, and heavy rainfall in Bangkok and Chiang Mai during the period from 15 April to 15 June, 1998.

In this study, the onset of monsoon is deter-

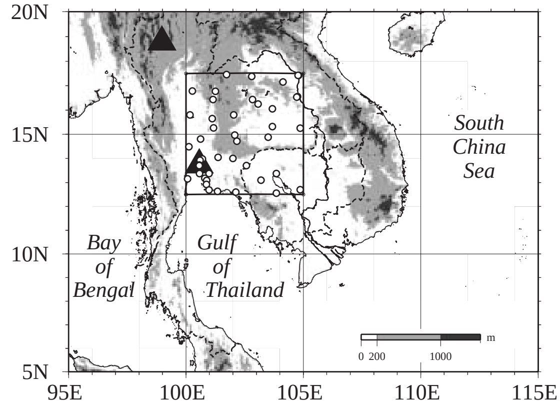

Fig. 1. Map of the study area. Light and dark shadings indicate elevations higher than 200 and 1000 m, respectively. Open circles are the rainfall stations, and black triangles are the GPS stations used in this study. Northern and southern one indicate Chiang Mai and Bangkok, respectively.

mined by the time series of zonal wind at 850 and 700 hPa, which will be elaborated in Section 3. Furthermore, the evolution of the spatial distribution of pentad mean OLR and wind at 850 hPa are used. Wind data are obtained by the daily mean values of the reanalysis of the National Centers for Environmental Prediction/National Center for Atmospheric Research (NCEP/NCAR) (Kalnay et al. 1996). As an indicator of the convective activity, the daily mean interpolated OLR data provided by the National Oceanic and Atmospheric Administration (NOAA) are utilized. The temporal and spatial interpolation method is noted by Liebmann and Smith (1996). The spatial resolution for both data is 2.5 degree. The pentad mean OLR, and wind at 850 hPa, are calculated using these daily mean data. In Section 4, the atmospheric conditions causing the convective activity before the summer monsoon onset using daily mean reanalysis data are investigated.

In this study, the pre-monsoon period over the Indochina Peninsula is defined as a period from March to the monsoon onset date, determined by the establishment of monsoon circulation, as will be shown in the next session. The main study area is in the central area of the Indochina Peninsula (12.5°–17.5°N, 100°–105°E), shown by a square in Fig. 1.

3. Rainfall during the pre-monsoon period

Orgill (1967) defined the onset of the southwest monsoon over Southeast Asia as the lower tropospheric equatorial westerlies move northward into southern China. Operationally, the onset of southwest monsoon over this region is sometimes defined as zonal wind components at both 850 and 700 hPa become positive, and stay positive at least 20 days after that date (e.g., Cheang and Tan 1988). This method is used in this study.

Figure 2a shows the time series of the area averaged daily mean zonal wind around the central area of the Indochina Peninsula from March to June in 1998. We can see that the zonal winds at 850 hPa and 700 hPa layers for the March–May period have similar characteristics. In March and April, they show positive (indicating westerly) or negative (indicating easterly) value almost concurrently. In con-

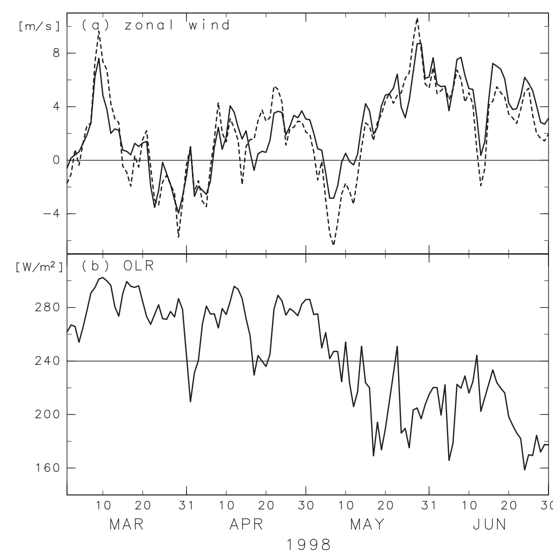

Fig. 2. The time series of the area averaged daily mean (a) zonal wind (m s^{-1}) and (b) OLR (W m^{-2}), respectively, from March to June in 1998. (a) The thick line and the broken line are zonal wind at 850 hPa and 700 hPa, respectively. (b) Horizontal line means the threshold value for strong convective activity, 240 W m^{-2}.

trast, they become positive (westerly) and stay positive more than 20 days after 14 May. Based on the above result, the monsoon onset in the central region of the Indochina Peninsula is defined to occur on 14 May in 1998.

To validate the monsoon onset determined by the above definition, the expansion of the convective activity using OLR data is checked. Figure 2b shows the time series of the daily mean OLR in the central area of the Indochina Peninsula from March to June in 1998. The threshold value less than 240 W m^{-2} is used, indicating strong convective activity. The OLR value becomes less than this value in middle May. After that, strong convective activity, indicated by the value less than 240 W m^{-2}, is roughly maintained. In contrast, there are several strong convective events intermittently in April and early May. The continuous strong convective activity starts in middle May in conjunction with the monsoon onset. As a result of an inspection of both panels in Fig. 2, the monsoon onset starts on 14 May. The rainfall brought about before this date, hereafter, will be called pre-monsoon rain.

To indicate the change of the circulation in the lower atmosphere associated with the monsoon onset, the pentad mean wind field at 850 hPa, from 6 May to 30 May in 1998, is composed (Fig. 3). In pentad number (hereafter referred to as the 'Pn') 26 (6–10 May, Fig. 3a) and 27 (11–15 May, Fig. 3b), the strong westerly is located in the northern part of India and the Indochina Peninsula, as a part of the mid-latitude westerly belt. On the other hand, the easterly trade wind associated with the western Pacific subtropical high reaches the Bay of Bengal. The Indochina Peninsula is located in a boundary area between the mid-latitude westerly and the easterly trade wind. The equatorial westeries still stay around the equatorial Indian Ocean. In Pn 28 (16–20 May, Fig. 3c), the strong southwesterly reaches over the southern part of the Indochina Peninsula and the northern part of the South China Sea from the equatorial region of the Indian Ocean. In contrast, the easterly trade wind associated with the western Pacific subtropical high retreats eastward to the western Pacific Ocean. Moreover, the mid-latitude westerly retreats northward (not shown). After Pn 29 (21–25 May, Fig. 3d), the whole Indochina Peninsula is controlled by the southwesterly monsoon flow. The seasonal march around the monsoon onset in 1998 is very similar to the result shown as the composite pentad mean 850 hPa wind field shown by Zhang et al. (2002). On the monsoon onset, the trade wind and mid-latitude westerly retreat eastward and northward, respectively, and the equatorial westerly flow from the Bay of Bengal extends to the South China Sea.

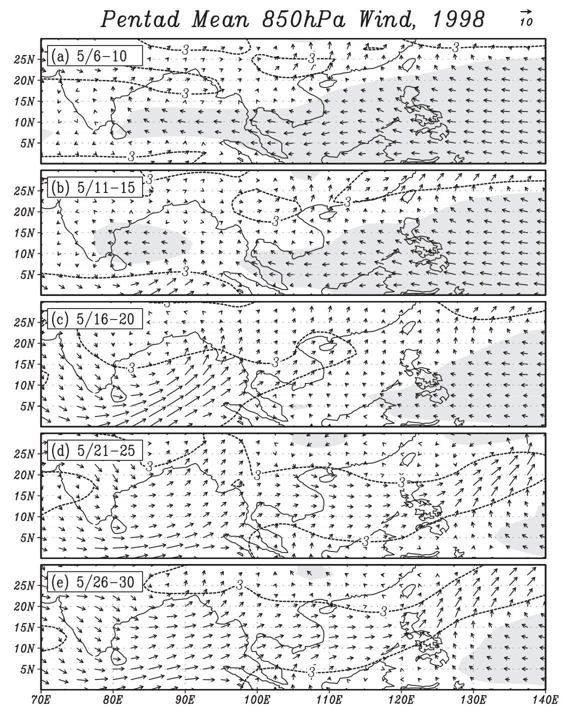

Fig. 3. Evolution of pentad mean wind field at 850 hPa in units of m s^{-1} in 1998. The dashed line means the contour of 3 m s^{-1} zonal wind. Shadings indicate the regions of less than -3 m s^{-1} zonal wind. (a) 6–10 May (Pn 26), (b) 11–15 May (Pn 27), (c) 16–20 May (Pn 28), (d) 21–25 May (Pn 29) and (e) 26–30 May (Pn 30).

In addition to Fig. 3, the evolution of the convective activity indicated by OLR in the same period is shown (Fig. 4). In Pn 26 (Fig. 4a), the lower OLR regions (which represents the heavy convective activity) appear over the southern part of the Bay of Bengal, the maritime continent and the equatorial region of the West Pacific Ocean. Around the Indochina Peninsula, the lower OLR area extends from

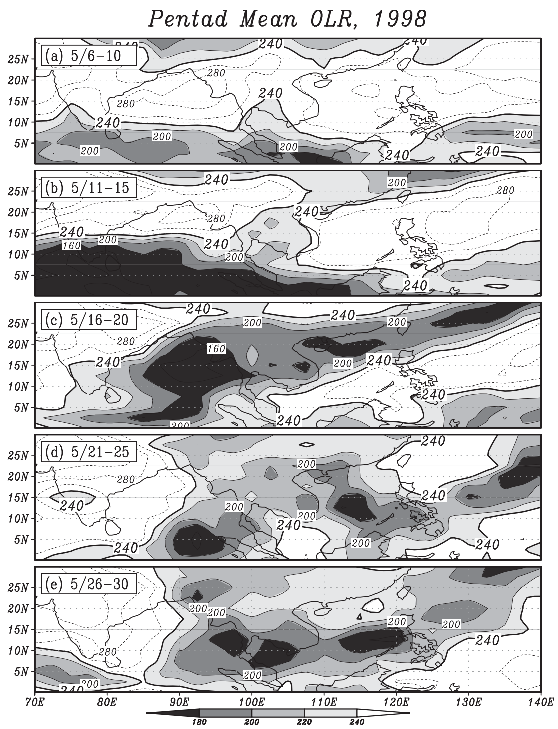

Fig. 4. Same as Fig. 3, but for the OLR in units of W m^{-2}. The contour interval is 20 W m^{-2}. The thick bold line indicates the contour of 240 W m^{-2}, the threshold value of the strong convective activity. Contour lines exceeding 260 W m^{-2} are in broken lines. Shadings indicate the regions of less than 240 W m^{-2}. (a) 6–10 May (Pn 26), (b) 11–15 May (Pn 27), (c) 16–20 May (Pn 28), (d) 21–25 May (Pn 29) and (e) 26–30 May (Pn 30).

the low-latitude zone to the southern part of the Indochina Peninsula. Meanwhile, two higher OLR regions (which indicate the suppressed convective activity) are located over the Bay of Bengal and the South China Sea. During the period around the monsoon onset (Pn 27 and 28, Figs. 4b and 4c), the expansion of the lower OLR area over the Indochina Peninsula is ahead of that over the Bay of Bengal and the South China Sea, then the strong convection over the whole region, from the Bay of Bengal to the South China Sea occurs. After the monsoon onset (Pn 29, Fig. 4d), the whole Indochina Peninsula and the South China Sea is covered by the lower OLR region. In contrast, the region from the western part of the Bay of Bengal to the Indian subcontinent is still under the suppressed convective activity. In Pn 30 (Fig. 4e), the strong convection continuously covers the eastern part of the Bay of Bengal, the Indochina Peninsula and the South China Sea. Meanwhile, the Indian subcontinent and the equatorial region of the West Pacific Ocean are still under the higher OLR area. This result of seasonal changes of convective activity in 1998 is consistent with that by He et al. (1987), Matsumoto (1992), Hirasawa et al. (1995), and Zhang et al. (2002), which recognized large-scale abrupt seasonal changes in this period over the Indochina Peninsula.

According to Fig. 2b, the intermittent decreases of the OLR are observed during the pre-monsoon period. Figure 5b shows the time series of the area averaged station precipitation (using 44 stations shown in Fig. 1) for the period from March to May 1998. The intermittent rainfall events during the pre-monsoon period are seen in early March (marked by A), from late March to early April (marked by B, and C), in middle April (marked by D) and early May (marked by E). Up to now, such intermittent rainfall events over the Indochina Peninsula have not been pointed out, except for the climatological description by Nieuwolt (1981). He noted that the local convection produced by thunderstorm is rather active in April. According to the distribution of precipitation (not shown), however, rainfalls occur in wide area of research domain in these rainfall events.

Then, to investigate the large-scale characteristics of the rainfall phenomena during the pre-monsoon period, the time-latitude section of the daily mean OLR from March to May in 1998 is shown (Fig. 5a). In early April, middle April and early May during the pre-monsoon, the lower OLR regions marked by a to c extend southward from the mid-latitude zone to the Indochina Peninsula. The interval of these southward extensions is about 10–20 days. After the last intermittent convective activity (marked c), we can see that the lower OLR region migrates northward from the low-latitude zone to the Indochina Peninsula in middle May. Then, the major part of the Indochina Peninsula is under OLR value lower than 240 W m^{-2}, indicating enhanced convective activities accompanied with the monsoon.

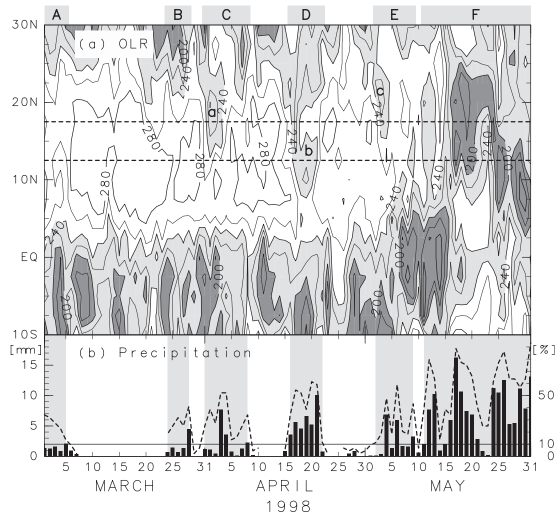

Fig. 5. (a) The time-latitude cross sections of the daily mean OLR along 100°–110°E, and (b) the time series of area averaged rainfall (black bar) and the ratio of the stations where rainfall is observed (dashed line) based on the daily rainfall amount at 44 stations shown in Fig. 1 from March to May in 1998. (a) The unit is W m^{-2}. The contour interval is 20 W m^{-2}. Light and dark shadings are less than 240 and 220 W m^{-2}, respectively. Study area is located between 12.5° and 17.5°N, as shown by the two broken lines. Letters a, b, and c indicate the southward extension of the lower OLR region from the mid-latitude zone to the Indochina Peninsula. (b) The dashed line in the non-rain days is neglected. Unit of the rainfall and the ratio are mm day^{-1} and %, respectively. The shadings indicate the periods when the ratio of the stations where rainfall is observed exceeding 10%.

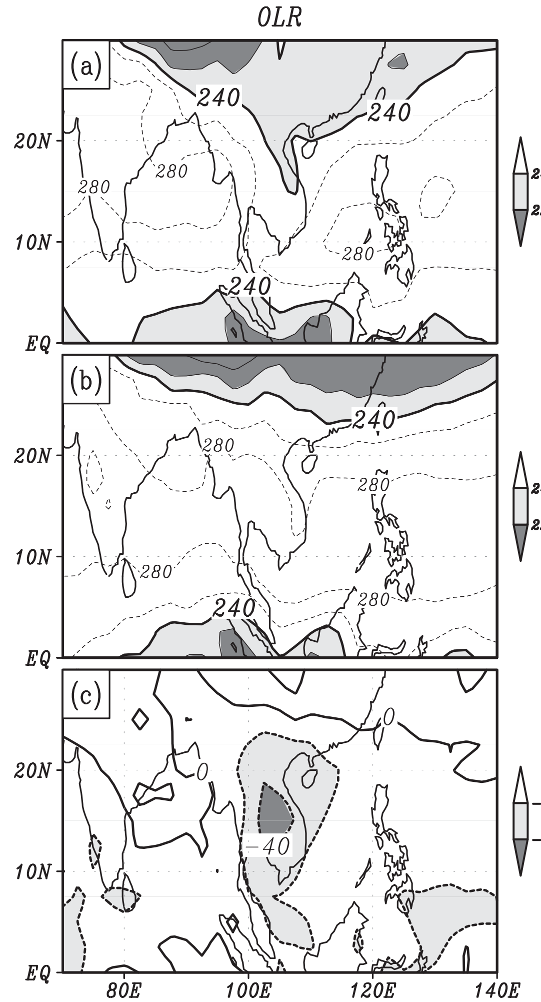

Fig. 6. Composites of OLR for (a) rain periods C, D and E, and (b) the non-rain days from March to mid-May, 1998. The bottom panel (c) shows the difference between (a) and (b). The difference is calculated by subtracting (b) from (a). The unit is W m^{-2}. The contour interval is 20 W m^{-2}. Light and dark shadings of (a) and (b) are less than 240 and 220 W m^{-2}, respectively. Light and dark shadings of (c) are less than −20 and −40 W m^{-2}, respectively.

In order to show the spatial property of these intermittent convective activities, the composite analysis is carried out. Figures 6a and 6b show the composite map of OLR in the rain days (when the ratio of the stations with observed rainfall exceeding 0 mm is exceeding 10%) during the periods C, D, and E, and the non-rain days (when there is no station with observed rainfall) from March to mid-May, respectively. Figure 6c shows the difference between the composite of the rain days and the non-rain days. The number of rain days (during the periods C, D, and E), and non-rain days (during the period from March to mid-May), are 24 days and 21 days, respectively.

On the rain days (Fig. 6a), the region of OLR value less than 240 W m^{-2} extends southward from the mid-latitude zone to the

Indochina Peninsula. The central area of the Indochina Peninsula is under OLR value less than 260 W m^{-2}. In contrast, the Indian subcontinent, the Bay of Bengal, and the southern part of the South China Sea are under the higher OLR region, indicating the suppressed convection. The difference shown by Fig. 6c can more clearly indicate the property shown above. A negative area indicating more activated convective activity covers from the southern coast of China to the central area of the Indochina Peninsula.

In order to investigate where the intermittent convection comes from, daily OLR fields are composed based on the first day of the rain events in periods C, D, and E (Fig. 7). The first day of the rainfall events is denoted as day 0, while the sign of '$-$' and '$+$' denote prior to and after the first day of the rainfall events, respectively. Before -3 day, the lower OLR region (OLR < 240 W m^{-2}) does not appear over the Indochina Peninsula. On -2 day, the lower OLR region appears in the northwest of the Bay of Bengal. Then, this convective region moves eastward. On -1 day, there occurs strong convection around Bangladesh. On the first day of the rainfall events (0 day), the lower OLR region extends southward over Vietnam, Laos, and the inland area of Thailand. The lower OLR region is more strengthened in the central region of Thailand, Laos, and Vietnam on $+1$ day. In addition, a band like strong convective activity over the Indochina Peninsula is extended to the southern coast area of China. The strong convection stays over the Indochina Peninsula and the southern coast region of China from $+2$ day to $+4$ day. However, the center of this convection area gradually moves away from the Indochina Peninsula to the southern part of China. In contrast, the higher OLR region covers the west coastal region of the Indochina Peninsula for the whole period from -5 day to $+4$ day.

From the above composite analysis, it is shown that the strong convective activity area migrates eastward from the northwest of the Bay of Bengal to the northeastern part of the Indochina Peninsula, along the southeastern edge of the Tibetan Plateau. Then, the convective activity extends southward to the Indochina Peninsula. After that, the convective activity covers from the Indochina Peninsula to the southern coastal area of China, forming a band shape extending from northeast to southwest.

Up to now, the rainfall during the premonsoon period was recognized as local phenomena generated in local area in climatological descriptions (Nieuwolt 1981). However, it is shown that the organized intermittent convective activities are not generated in the Indochina Peninsula, but migrate eastward from the west of the Indochina Peninsula. That is, these intermittent convective activities are regarded as synoptic phenomena. The large-scale situations related with these rain events will be further investigated in the next session.

4. Synoptic conditions related with pre-monsoon rainfall events

4.1 Seasonal march of vertical profile of air temperature

Figure 8a shows the vertical-time cross section of area averaged temperature anomaly, from the annual mean in the central area of the Indochina Peninsula, from March to May, 1998. It can be seen that the cold air in the upper troposphere appears in early and late March, labeled by A and B in Fig. 8a. It is suggested that the inflow of cold air in the upper troposphere has some affect on the convective activity. Meanwhile, the cold air in the upper troposphere appears in rain events during the pre-monsoon period, marked by C, D and E, is weaker than that in periods A and B.

On the other hand, the temperature in the lower troposphere decreases in the rain events during the whole pre-monsoon period. It is suggested that the decrease of temperature is produced by the evaporation of raindrops and the interception effect of sunshine by cloud. The rise of temperature produced by the release of latent heat in the upper troposphere after the monsoon onset on 14 May is noted.

From the above analysis, there is the presence of cold air in the upper troposphere in the rain events in March. In the rain events in April, the presence of the cold air in the upper troposphere becomes not very clear. It is suggested that the release of latent heat by the condensation associated with convection have no smaller affects on the temperature in the upper troposphere, even in the pre-monsoon season. The rise of temperature in the upper

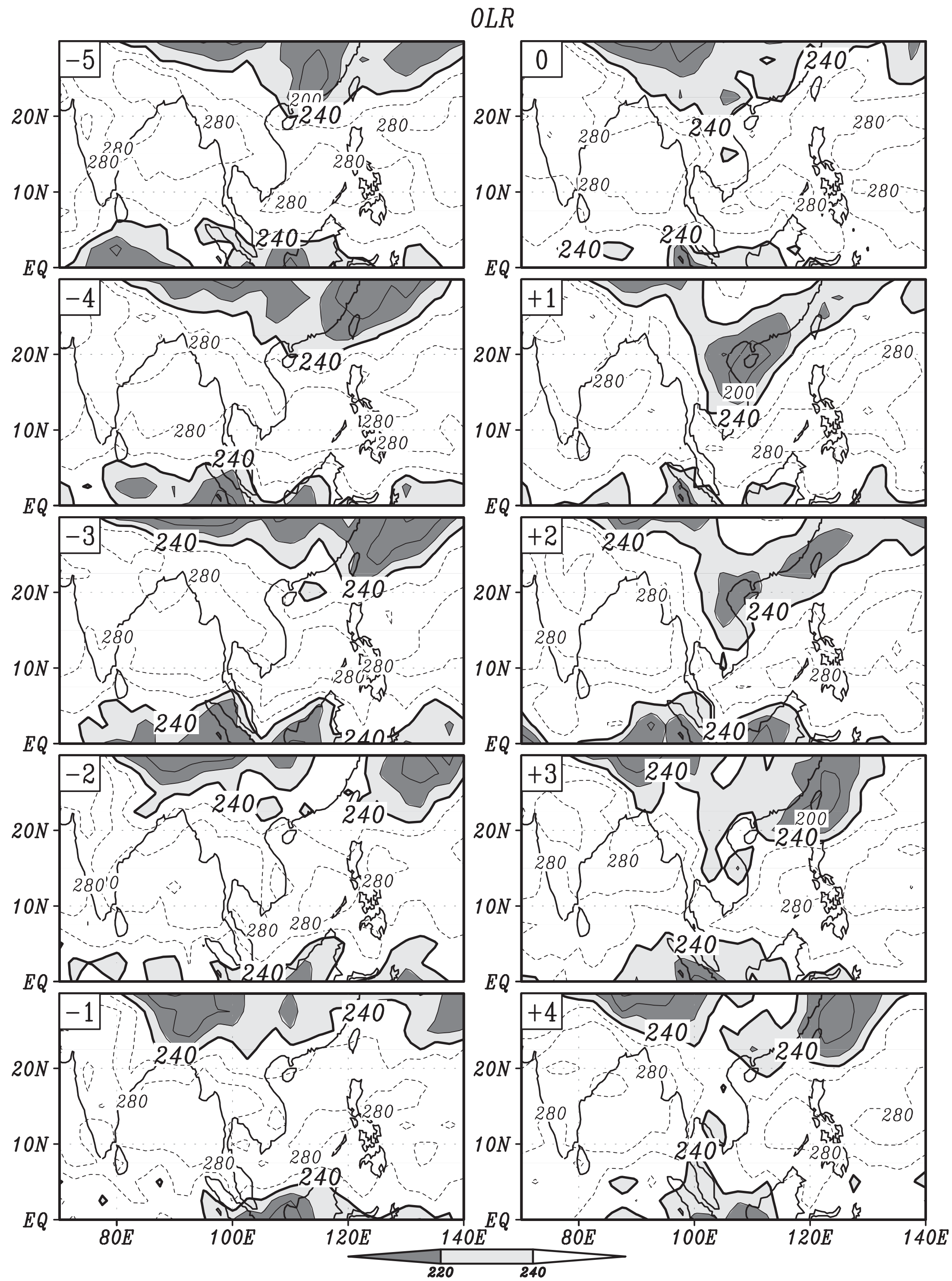

Fig. 7. Daily evolution of the composite OLR with reference to the first day of the strong convective activity periods (C, D, and E). Here '0' denotes the first day of the strong convective activity periods C, D, and E. '−' and '+' refer to prior to and after the first day of the strong convective activity periods (C, D, and E), respectively. The unit is W m^{-2}. The contour interval is 20 W m^{-2}. Light and dark shadings are less than 240 and 220 W m^{-2}, respectively.

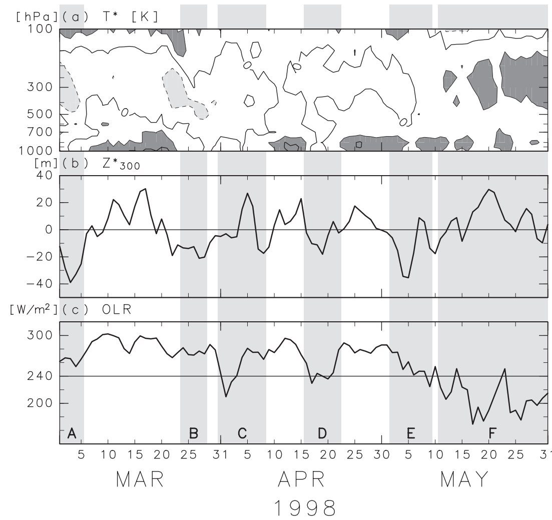

Fig. 8. (a) The vertical-time cross section of area averaged mean temperature anomaly from the annual mean value (°C), (b) the time series of area averaged mean 300 hPa height anomaly from the 30-day running mean value (m), and (c) OLR (W m^{-2}) in the central region of the Indochina Peninsula (12.5°–17.5°N, 100°–105°E) from March to June in 1998. The contour interval of (a) is 1°C. Light and dark shadings of (a) are less than −2°C and more than 2°C, respectively. Shadings in the above and below (a) indicate the periods when the rainfall events occur, which are defined in Section 3.

troposphere is more noted after the monsoon onset.

4.2 *The trough passages in the upper troposphere*

As a factor for generating convective activity, we can point out the passage of trough in the upper troposphere that may bring an inflow of cold air in the upper troposphere, and the upward flow in the troposphere. Thus, the temporal changes of geopotential height field at 300 hPa layer are analyzed. Figure 8b shows the time series of the 300 hPa geopotential height anomaly from the 30-day running mean. The seasonal change can be ignored by using the anomaly from the 30-day running mean value. The troughs appear during the rainy events in the pre-monsoon period (A, B, D and E). A trough is not very clear during the period C, when the trough passes more northward (not shown). During the periods C and D, the presence of cold air (Fig. 8a) is concurrent with the trough passage in the upper troposphere (Fig. 8b). In order to reveal the property of convective activity at the passage of trough in the upper troposphere, the time series of the area averaged OLR value (Fig. 8c) is shown. During the periods C, D, and E, the OLR value is below 240 W m^{-2}, indicating strong convection. In spite of the appearance of the trough and the rainfall, the OLR value during the periods A and B is not below 240 W m^{-2}. It is indicated that the convection during the periods A and B is weaker than that during the periods C, D and E. Thus, it is clarified that there is a difference in the property of OLR between the periods A and B, and periods C, D and E.

Figure 9 shows the composite map of wind field at 300 hPa layer on the rain events (a), on the non-rain days during the period from March to the monsoon onset (b), and the difference between the two (c). The trough at 300 hPa stretches from Myanmar to the eastern Bay of Bengal, that is in the west of Thailand, on rain events. In contrast, on non-rain days, the strong westerly jet appears over the northern part of the Indochina Peninsula, and troughs are not observed around the Indochina Peninsula. The difference between the rain events and the non-rain days shows that there is a cyclonic anomaly over the Indochina Peninsula, indicating the presence of the trough.

In order to show the migration of the trough in the upper troposphere associated with the rainfall events, daily wind circulation at 300 hPa is composed, shown in Fig. 10, as well as the composite analysis of OLR field (Fig. 7). Before −3 day, the strong westerly jet appears over the northern part of the Indochina Peninsula. On −2 day, the trough appeares in eastern India, nearby 80°E. Then this trough moves eastward. On the first day of the rainfall events, this trough reaches Myanmar. From +1 day to +4 day, this trough crosses over the Indochina Peninsula from west to east. It is shown that this trough is generated in eastern India.

To reveal the change of the vertical circulation associated with the trough passage in the upper troposphere, the relation between the

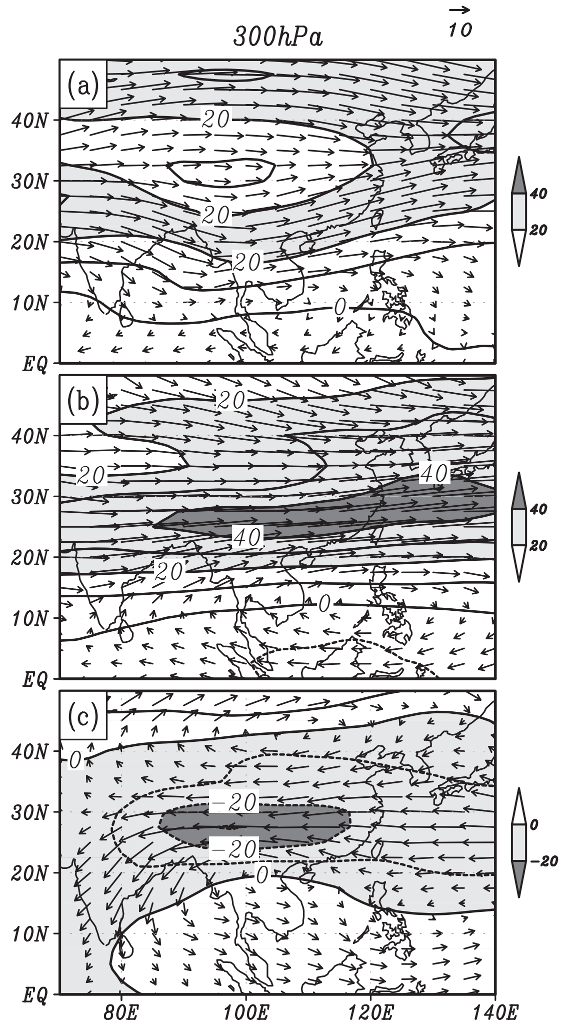

Fig. 9. Same as Fig. 6, but for the 300 hPa wind vector and the zonal wind speed. Contour interval is 10 m s^{-1}. Light and dark shadings in (a) and (b) are more than 20 m s^{-1} and more than 40 m s^{-1}, respectively. Light and dark shadings of (c) are less than 0 m s^{-1} and less than -20 m s^{-1}, respectively.

anomalous geopotential height and the upward flow (ω) is shown. Figure 11 shows the vertical-time cross section of the anomalous geopotential height and ω. The upward flow is strengthened when the anomalous geopotential height is negative, indicating the trough passage during the pre-monsoon period. In contrast, the trough passages and upward motion are not coincident after the monsoon onset (during the period F). Therefore, it can be said that the upward flow associated with the trough passages in the upper tropospheric westerlies during the pre-monsoon period is strengthened over the central part of the Indochina Peninsula.

From the above analysis, the convection during the periods A and B is produced by the strengthening of the upward motion, and the presence of cold air associated with the trough passage in the upper troposphere. In the research domain, the OLR value during the periods A and B is larger than that during the periods C, D and E. Two causes of this situation are thought. One is that the altitude of cloud top is lower. Another is that there is a small amount of cloud. The GMS (geostationary meteorological satellite) images during the periods A and B are checked, and it is thought that the cause of this situation is a small amount of cloud in the research domain (not shown). During the periods C, D and E, there is the trough passage same as during the periods A and B. But the decrease of temperature in the upper troposphere is not clear. It is clarified that the trough in the upper troposphere moves eastward along the southern edge of the Tibetan Plateau.

4.3 Moisture convergence in the lower troposphere

The convergence of moisture is indispensable for the convective activity that brings precipitation. Therefore, the distribution and transportation of moisture are examined. Figure 12a shows the time series of the vertical integration of the precipitable water, using the daily mean specific humidity data by NCEP/NCAR. The vertical integration W is given by

$$W = \int_{p_{1000}}^{p_{300}} q \frac{dp}{g} \tag{1}$$

where W, p_{1000}, p_{300}, q, and g represent precipitable water, pressure at 1000 hPa layer, pressure at 300 hPa layer, specific humidity and gravity acceleration, respectively. Figure 12b shows the time series of the precipitable water at Bangkok (solid line) and Chiang Mai (thick line) derived from GPS observations. GPS observations begin from April in 1998.

The change trends of these two kinds of the precipitable water are similar, except for the

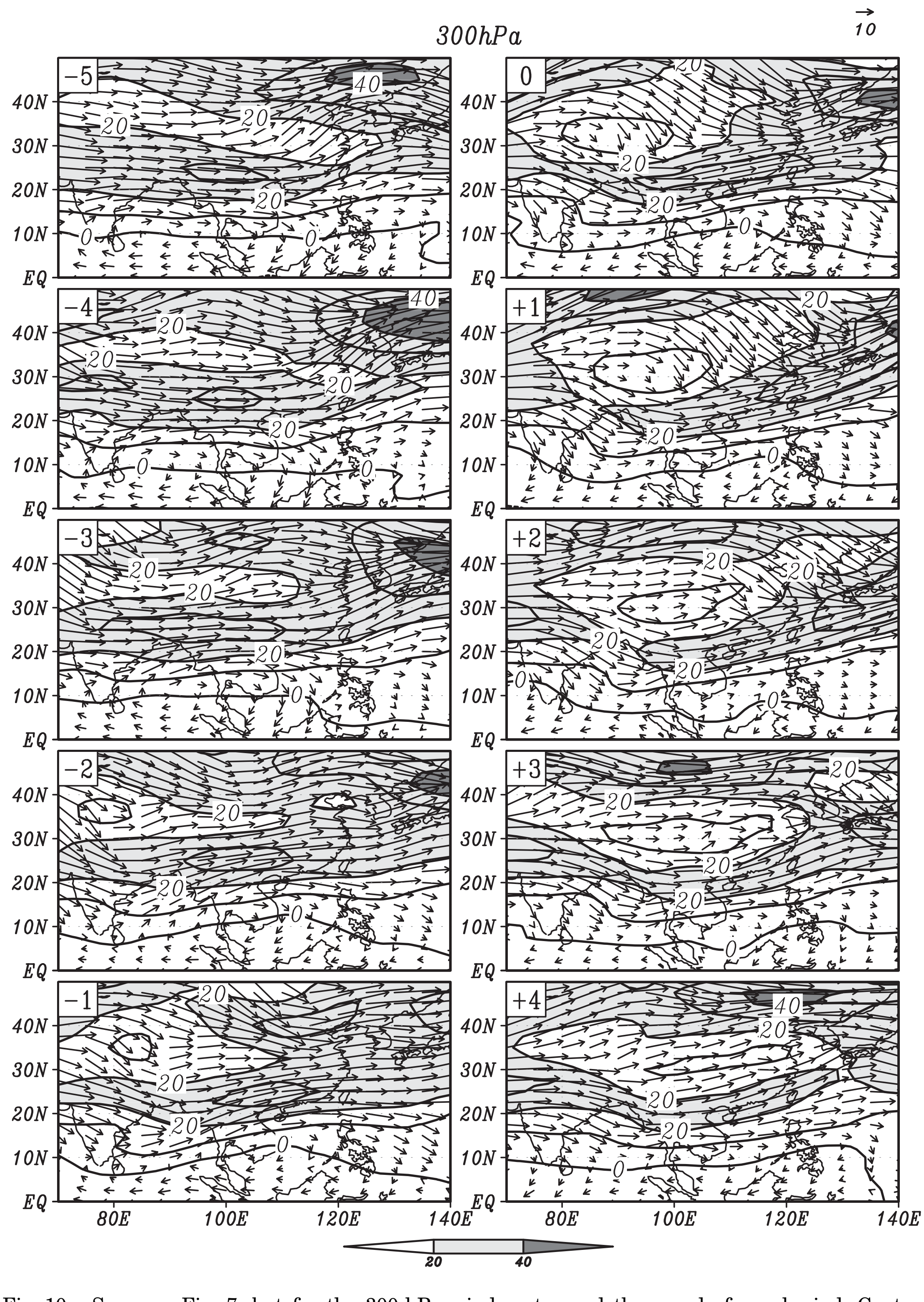

Fig. 10. Same as Fig. 7, but for the 300 hPa wind vector and the speed of zonal wind. Contour interval is 10 m s^{-1}. Light and dark shadings are more than 20 and more than 40 m s^{-1}, respectively.

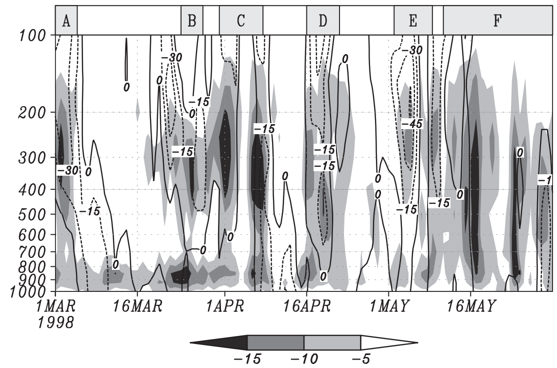

Fig. 11. The vertical-time cross section of height anomaly from the 30-day running mean value (contoured) and ω (shaded) at 15°N, 102.5°E for the period from March to May in 1998. The unit of height anomaly and ω are m and 10^{-2} Pa s^{-1}, respectively. Contour interval of height anomaly is 15 m only for negative value. Shading is less than -5×10^{-2} Pa s^{-1}. Shading interval is 5×10^{-2} Pa s^{-1}. Shadings in the upper part of the figure indicate the periods when the rainfall events occur, which are defined in Section 3.

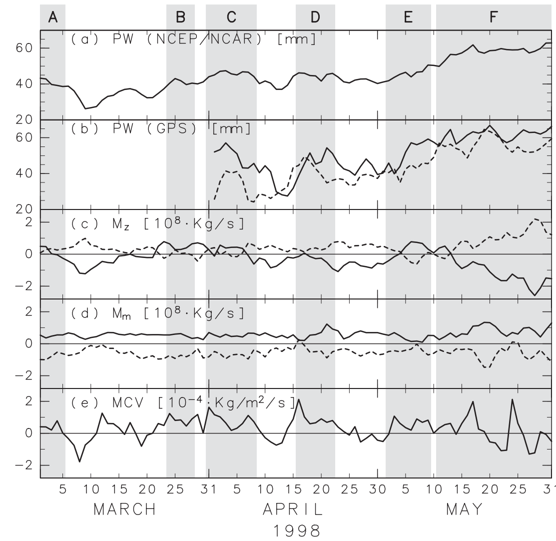

Fig. 12. The time series of area averaged value of (a) the vertical integration of the precipitable water using the NCEP/NCAR reanalysis data, (b) the precipitable water derived from GPS observations at Bangkok (thick line) and Chiang Mai (broken line), (c) the vertical integration of the zonal moisture inflow between 12.5°N and 17.5°N along 105°E (thick line) and 100°E (broken line), (d) the vertical integration of the meridional moisture inflow between 100°E and 105°E along 12.5°N (thick line) and 17.5°N (broken line), (e) the vertical integration of the moisture convergence in the central area of the Indochina Peninsula (12.5°–17.5°N, 100°–105°E). The periods of (a), (c), (d), and (e) is from March to May in 1998. The data of the precipitable water derived from GPS observation is shown during the period from April to May in 1998. The unit of (c) and (d) is 10^8 Kg s^{-1}. The unit of (e) is 10^{-4} Kg m^{-2} s^{-1}. Shadings indicate the periods when the rainfall events occur, which are defined in Section 3.

magnitude of oscillations. So, it is judged to be all right to discuss the increase and decrease of moisture using the reanalysis data. The precipitable water increases ahead of the periods B, C, D and E. On the other hand, the precipitable water decreases after the periods A, B, C and D. In contrast, the precipitable water does not decrease after the period E, and the moisture amount increases continuously towards the monsoon onset on 14 May. In addition, although the precipitable water slightly increases in middle March between the periods A and B, there are no rainfall events during this period. During this period, there are no trough passages in the upper troposphere and OLR decreases a little (Figs. 8b and 8c), and the convection in middle March between the periods A and B, does not become strong enough to bring large-scale rainfall.

To reveal the origin of moisture supplied to the research domain during the rain events, first of all, the time series of moisture fields in the central area of the Indochina Peninsula are shown. Figures 12c and 12d show the time series of the vertically integrated moisture inflow from the east (solid line), west (thick line), south (solid line), and north (thick line). From the time series of vertically integrated moisture inflow from each direction, the relationship between the moisture inflow from the east, and rain events is focused. The moisture inflow from the east is positive during the periods A, B, C, and E. The moisture inflow from the west and east becomes weak for the period D. In contrast, the moisture inflow is mainly from the west and south during the period F. On the other hand, the meridional moisture inflow is almost from the south during the period from March to May.

Figure 12e shows the time series of the vertically integrated moisture convergence in the study area. There is the strengthening of moisture convergence before the appearance of strong convection for the periods B, C and D. On the other hand, moisture convergence is not observed before the period E. However, the moisture inflow from the east increases rapidly when the period E starts, and moisture convergence is strengthened. This is simultaneous with the trough passage in the upper troposphere (Fig. 8b). In addition, as well as the increase of precipitable water (Figs. 12a and 12b), moisture convergence is strengthened in middle March, and there are no rainfall events in this period (Fig. 5b). It is thought that the strengthening of moisture convergence produces the increase of precipitable water. As shown in the above analysis, it is seen that the moisture convergence during the rain events is brought by the moisture inflow from the east and south.

To reveal the moisture inflow from which direction contributes to the intermittent rainfall events during the pre-monsoon period quantitatively, the composite analysis of the vertically integrated moisture inflow into the study area from each direction is carried out. Figure 13 shows the composite map of the vertically integrated moisture inflow during the rain events (periods C and D) (a), and on non-rain days for the period from March to the monsoon onset date (b), respectively. According to the above composite analysis, it is clarified that moisture convergence becomes strengthened on the rain events. In contrast, Fig. 13b indicates that there is moisture divergence on non-rain days. The moisture inflow from the south and north is almost the same amount in both rain events (Fig. 13a) and non-rain days (Fig. 13b). But the characteristics of the inflow from the zonal direction are drastically different between them. On non-rain days, the amount of moisture outflow to the east is higher than that of moisture inflow from the west. Although the amount of moisture inflow is different, such characteristics are similar to those after the monsoon onset (Fig. 13c).

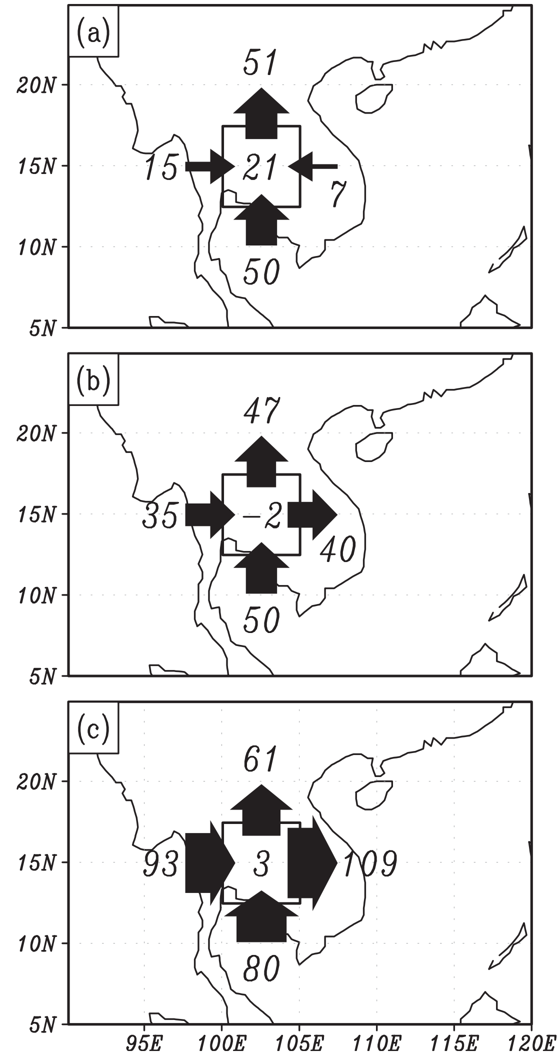

Fig. 13. Composites of the vertical integration of zonal and meridional moisture fluxes passing across boundaries of the box (12.5°–17.5°N, 100°–105°E) and the precipitable water in this box in (a) the periods C, D and E, (b) the non-rain days from March to May, and (c) the period F. Arrows indicate the direction of flux. The numeral written in the center of the box is the amount of precipitable water in the box. The unit of the moisture flux and that of the precipitable water are 10^6 Kg s^{-1} and 10^6 Kg m^{-2}, respectively.

To investigate the atmospheric circulation field related to the strengthening of easterly

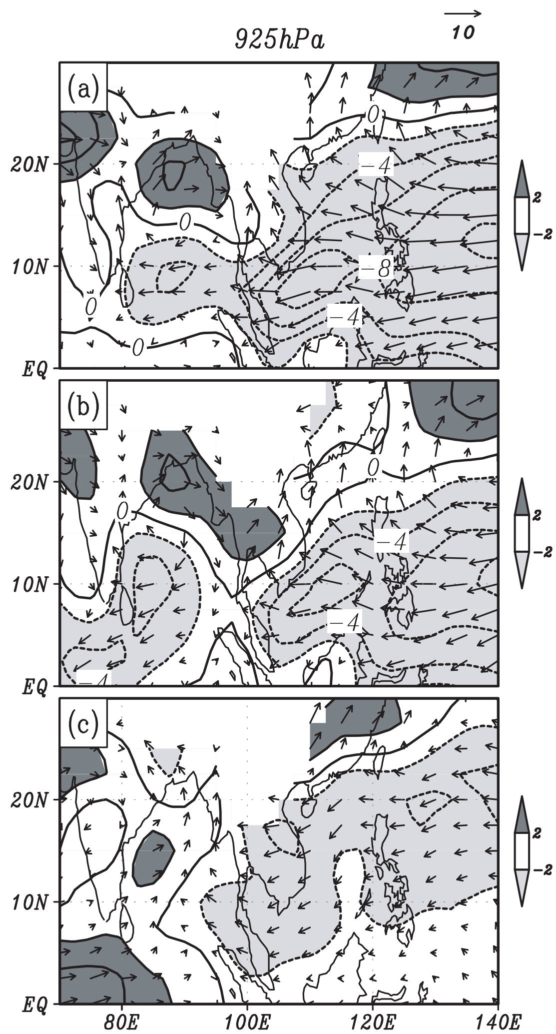

Fig. 14. Same as Fig. 6, but for the 925 hPa wind vector and the zonal wind speed. Contour interval is 2 m s^{-1}. Light and dark shadings are less than -2 m s^{-1} and more than 2 m s^{-1}, respectively.

moisture inflow, the composite map of the wind field at 925 hPa is constructed on rain events (Fig. 14a). The line indicating the boundary between the westerly and easterly is located at approximately 100°E on rain events. It is clear that the southeasterly flows into the inland region of the Indochina Peninsula. In contrast, the westerly is dominant over the Indochina Peninsula on non-rain days (shown in Fig. 14b). The features on rain days are shown more clearly by taking the difference between (a) and (b) (Fig. 14c). The anomalous easterly on rain events covers from the western North Pacific Ocean to the Indochina Peninsula.

Furthermore, in order to show the evolution of strengthening of easterly from the western North Pacific Ocean to the Indochina Peninsula, the composite analysis based on the first day of the period of the rain events (periods C, D and E) is carried out (Fig. 15). On -5 day, easterly from the South China Sea blows only in the southeastern tip of the Indochina Peninsula. The westerly from the Bay of Bengal covers the central part of the Indochina Peninsula. On -1 day, the easterly extends northwestward a little. As a result, the boundary of the easterly and westerly is located in the central area of the Indochina Peninsula. After 0 day, the easterly from the South China Sea becomes strengthened north of 10°N.

5. Concluding remarks

In this study, the property atmospheric conditions associated with the rainfall events during the pre-monsoon period are investigated in the GAME-IOP year, 1998. The monsoon onset is defined as that zonal wind components become positive, and stay positive at least 20 days after that date at both 850 hPa and 700 hPa. The monsoon onset date in 1998, thus determined in the research domain, is 14 May. The intermittent precipitation events during the pre-monsoon period before this date are seen in early March, the period from late March to early April, middle April, and early May. In the rainfall events, rainfall is observed in wide area of the research domain. The strong convective activity extends southward from the mid-latitude zone to the Indochina Peninsula. These southward extensions are intermittent, and are in accordance with rainfall. The intermittent convective activities migrate eastward from the northwest of the Bay of Bengal to the northeastern part of the Indochina Peninsula, along the southeastern edge of the Tibetan Plateau. Then, the convective activities extend southward to the Indochina Peninsula. Up to now, the rainfall during the pre-monsoon period was recognized as local phenomena generated in a local area in climatological descriptions (Nieuwolt 1981). However, it is shown that the intermittent convective activities are not generated in the Indochina Peninsula, but

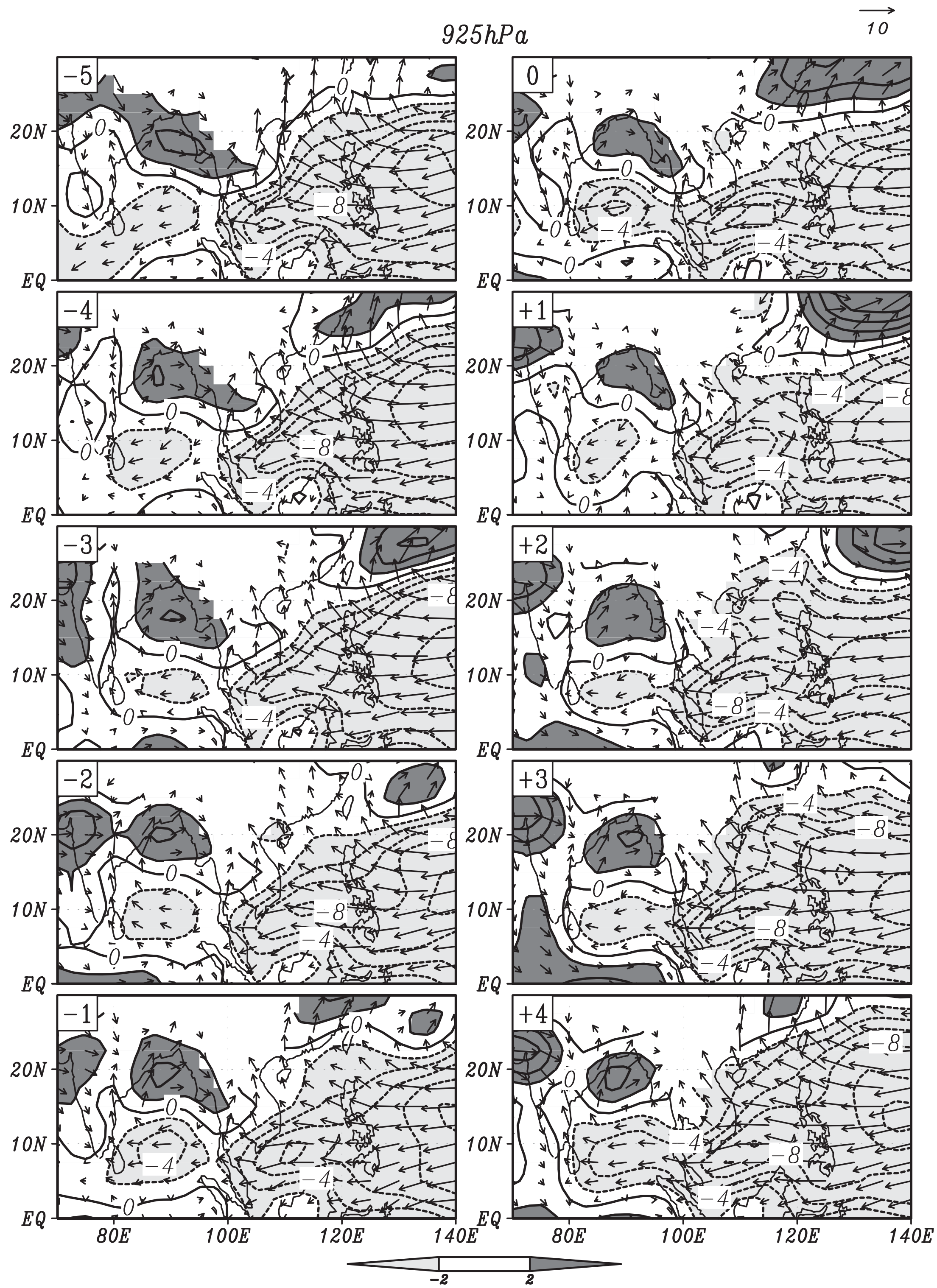

Fig. 15. Same as Fig. 7, but for the 925 hPa wind vector and the zonal wind speed. Contour interval is 2 m s^{-1}. Light and dark shadings are less than -2 m s^{-1} and more than 2 m s^{-1}, respectively.

migrates eastward from the west of the Indochina Peninsula. That is, this intermittent convective activities are synoptic phenomena.

The synoptic conditions associated with the intermittent rainfalls during the pre-monsoon period are the passage of the westerly trough in the upper troposphere, and the moisture inflow from the south and east in the lower troposphere. The westerly trough in the upper troposphere moves eastward along the southern edge of the Tibetan Plateau. Fujinami and Yasunari (2001) pointed out that the enhancement of the diurnal cloud activity period in spring is associated with a meandering of the jet stream over the Tibetan Plateau, with a trough over and to the south of the Tibetan Plateau, a weak wind speed through the troposphere over the Tibetan Plateau, and the cold air mass in the upper troposphere over the Tibetan Plateau. In the present study, the presence of cold air in the upper troposphere is not clear, causing the rainfall events during the pre-monsoon period in the central part of the Indochina Peninsula. However, the presence of the trough in the upper troposphere associated with the mid-latitude westerlies, are clearly shown in our study. It is thought that the uplift flow is strengthened when the trough in the upper troposphere advances southward to the Indochina Peninsula by the meandering of the mid-latitude westerlies. The boundary between the westerly and easterly in the lower troposphere is located in the central region of the Indochina Peninsula just before the rain events (on -1 day), and the easterly from the South China Sea is strengthened from the start of the rain events.

The analysis of this study was carried out only in 1998. To reveal the generality of the results, the investigation of rainfall during the pre-monsoon period for a longer period is needed. The speculation exists that the onset may be related to other aspects of climate, such as the overall strength of the monsoon season and ENSO (Joseph et al. 1994). It is important to reveal the relationship between the monsoon onset and other climate features such as ENSO.

Acknowledgments

Special thanks to Professors Tetsuzo Yasunari of the Hydrospheric Atmospheric Research Center (HyARC), Nagoya University and Katumi Musiake of Fukushima University, for providing many chances for progression in the GAME (GEWEX Asian Monsoon Experiment) and GAME-Tropics projects. Also thanks to Dr. Yasushi Agata at the Graduate School of Frontier Sciences, the University of Tokyo, for preparation of the database in the GAME-Tropics and invaluable advice. Thanks also to Dr. Koichi Masuda of the Frontier Research System for Global Change (FRSGC), for his valuable advice. They would also like to express their thanks to Mr. Takahiro Omata, the Graduate School of Science, the University of Tokyo, for helping the drawing of some figures.

The reanalysis data were provided by the National Centers for Environmental Prediction/National Center for Atmospheric Research. The rainfall data were provided by the Thai Meteorological Department, Department of Meteorology and Hydrology, Laos, and Department of Meteorology, Cambodia. The GPS data were provided by Prof. Mikio Satomura, the Institute of Geosciences, Shizuoka University, and Dr. Toshiyuki Nakaegawa, the Climate Research Department, the Meteorological Research Institute, Japan. The Grid Analysis and Display System (GrADS), GFD-DENNOU Library, and the Generic Mapping Tools (GMT) were used for drawing figures. Part of this study was financially supported by the Grant-in-Aid for Scientific Research from the Japanese Ministry of Education, Culture, Sports, Science and Technology (No. 11201202, 11201209, and 14204044), a research project at the Research Institute of Humanity and Nature entitled “Global Water Cycle Variation and the Current World Water Resources Issues and their Perspectives” and CREST (Core Research for Evolutional Science and Technology) of JST (Japan Science and Technology Agency).

References

Agata, Y. ed., 2002: GAME-Tropics Dataset CD-ROM, GAME Publication CD-ROM No. 4, Japanese Sub-committee for GAME-Tropics, Tokyo, Japan.

Ahmed, R., 1989: Probabilistic estimates of rainfall extremes in Bangladesh during the premonsoon season. *Indian Geogr. J.*, **64**, 39–53.

——— and S. Karmakar, 1993: Arrival and withdrawal dates of the summer mosnoon in Bangladesh. *Intl. J. Climatol.*, **13**, 727–740.

Ananthakrishnan, R. and M.K. Soman, 1988: The onset of the southwest monsoon over Kerala. *J. Climatol.*, **8**, 283–296.

Baral, K.N. and D. Mackerras, 1992: The cloud flash-to-ground frash ratio and other lightning occurrence characteristics in Kathmandu thunderstorms. *J. Geophys. Res.*, **97**, 931–938.

Cheang, B.-K. and H.-V. Tan, 1988: Some aspects of the summer monsoon in South-East Asia May to September 1986. *Aust. Meteor. Mag.*, **36**, 227–233.

Fasullo, J. and P.J. Webster, 2003: A hydrological definition of Indian monsoon onset and withdrawal. *J. Climate*, **16**, 3200–3211.

Fujinami, H. and T. Yasunari, 2001: The seasonal and intraseasonal variability of diurnal cloud activity over the Tibetan Plateau. *J. Meteor. Soc. Japan*, **79**, 1207–1227.

He, H.J., W. McGinnis, Z. Song, and M. Yanai, 1987: Onset of the Asian monsoon in 1979 and the effect of the Tibetan Plateau. *Mon. Wea. Rev.*, **115**, 1966–1995.

Hirasawa, N., K. Kato, and T. Takeda, 1995: Abrupt change in the characteristics of the cloud zone in subtropical East Asia around the middle of May. *J. Meteor. Soc. Japan*, **73**, 221–239.

Holland, G.J., 1986: Interannual variability of the Australian summer monsoon at Darwin: 1952–82. *Mon. Wea. Rev.*, **114**, 594–604.

Hsu, H.H., C.T. Terng, and C.T. Chen, 1999: Evolution of large-scale circulation and heating during the first transition of Asian summer monsoon. *J. Climate*, **12**, 793–810.

India Meteorological Department, 1943: *Climatological atlas for airmen*, India Meteorological Department, New Delhi, India, 100pp.

Joseph, P.V., J. Eisheid, and R.J. Pyle, 1994: Interannual variability of the onset of the Indian summer monsoon and its association with atmospheric features, El Niño, and sea surface temperature anomalies. *J. Climate*, **7**, 81–105.

Kalnay, E., M. Kanamitsu, R. Kistler, W. Collins, D. Deaven, L. Gandin, M. Iredell, S. Saha, G. White, J. Woollen, Y. Zhu, M. Chelliah, W. Ebisuzaki, W. Higgins, J. Janowiak, K.C. Mo, C. Ropelewski, J. Wang, A. Leetmaa, R. Reynolds, R. Jenne, and D. Joseph, 1996: The NCEP/NCAR 40-year reanalysis project. *Bull. Amer. Meteor. Soc.*, **77**, 437–471.

Koteswaram, P. and V. Srinivasan, 1958: Thunderstorms over Gangetic West Bengal in the pre-monsoon season and the synoptic factors favourable for their formation. *Indian J. Meteorol. and Geophys.*, **9**, 301–312.

Kurashima, A., 1959: General circulation and monsoon. *Kisetufuu (monsoon)*, Nemoto, J. et al., Eds., Chijin-Shokan, Tokyo, Japan, 201–283 (in Japanese).

Lau, K.M. and S. Yang, 1997: Climatology and interannual variability of the southeast Asian summer monsoon. *Adv. Atmos. Sci.*, **14**, 141–162.

Liebmann, B. and C.A. Smith, 1996: Description of a complete (interpolated) outgoing longwave radiation dataset. *Bull. Amer. Meteor. Soc.*, **77**, 1275–1277.

Matsumoto, J., 1992: The seasonal changes in Asian and Australian monsoon regions. *J. Meteor. Soc. Japan*, **70**, 257–273.

———, 1997: Seasonal transition of summer rainy season over Indochina and adjacent monsoon region. *Adv. Atmos. Sci.*, **14**, 231–245.

Murakami, T. and J. Matsumoto, 1994: Summer monsoon over the Asian continent and western North Pacific. *J. Meteor. Soc. Japan*, **72**, 719–745.

Nieuwolt, S., 1981: The climates of continental Southeast Asia, *Climates of Southern and Western Asia, World Survey of Climatology*, **9**, K. Takahashi, and H. Arakawa, Eds., Elsevier Scientific Publishing Company, Amsterdam-Oxford-New York, 1–66.

Orgill, M., 1967: *Some aspects of the onset of the summer monsoon over South East Asia*, Report to U.S. Army, Contact DA28–043–AMC–01303(E), Colorado State University, 75 pp.

Ramage, C.S., 1971: *Monsoon Meteorology*, International Geophysics Series, Vol. 15, Academic Press, 296 pp.

Rao, D.V. and P.N. Boothalingam, 1957: On forecasting the time of incidence of Nor'westers at Calcutta. *Indian J. Meteorol. and Geophys.*, **8**, 61–66.

Takiguchi, H., T. Kato, H. Kobayashi, and T. Nakaegawa, 2000: GPS observations in Thailand for hydrological applications. *Earth Planets Space*, **52**, 913–919.

Tanaka, M., 1992: Interseasonal oscillation and the onset and retreat dates of the summer monsoon over the east, southeast and western North Pacific region using GMS high cloud amount data. *J. Meteor. Soc. Japan*, **70**, 613–629.

Tao, S.Y. and L.X. Chen, 1987: A review of recent research on the East Asian summer monsoon in China. *Monsoon Meteorology*, C.P. Chang and T.N. Krishnamurti, Eds., Oxford University Press, 60–92.

Wang, B. and LinHo, 2002: Rainy season of the Asian–Pacific summer monsoon. *J. Climate*, **15**, 386–398.

———, ———, Y. Zhang, and M.-M. Lu, 2004: Definition of South China Sea monsoon onset and commencement of the East Asia summer monsoon. *J. Climate*, **17**, 699–710.

Webster, P.J., V.O. Magana, T.N. Palmer, J. Shukla, R.A. Tomas, M. Yanai, and T. Yasunari, 1998: Processes, predictability, and the prospects for prediction. *J. Geophys. Res.*, **103**, 14,451–14,510.

Wu, G. and Y. Zhang, 1998: Tibetan Plateau forcing and the timing of the monsoon onset over South Asia and the South China Sea. *Mon. Wea. Rev.*, **126**, 913–927.

Xie, A., Y. Chung, X. Liu, and Q. Ye, 1998: The interannual variations of the summer monsoon onset over the South China Sea. *Theor. Appl. Climatol.*, **59**, 201–213.

Yin, M.T., 1949: A synoptic-aerologic study of the onset of the summer monsoon over India and Burma. *J. Meteor.*, **6**, 393–400.

Zhang, Y., T. Li, B. Wang, and G. Wu, 2002: Onset of the summer monsoon over the Indochina Peninsula: Climatology and interannual variations. *J. Climate*, **15**, 3206–3221.